Fish & Shellfish Immunology 40 (2014) 32–39

Contents lists available at ScienceDirect

Fish & Shellfish Immunology

journal homepage: www.elsevier.com/locate/fsi

Full length article

Structural and functional characterization of a novel molluskan ortholog of TRAF and TNF receptor-associated protein from disk abalone (*Haliotis discus discus*)

Youngdeuk Lee [a, 1], Don Anushka Sandaruwan Elvitigala [b, d, 1], Ilson Whang [b, d, *], Sukkyoung Lee [b, d], Hyowon Kim [b, d], Mahanama De Zoysa [c], Chulhong Oh [a], Do-Hyung Kang [a], Jehee Lee [b, d, *]

[a] Korea Institute of Ocean Science & Technology, Ansan 426-744, Republic of Korea
[b] Department of Marine Life Sciences, School of Marine Biomedical Sciences, Jeju National University, Jeju Self-Governing Province 690-756, Republic of Korea
[c] College of Veterinary Medicine, Chungnam National University, Yuseong-gu, Daejeon 305-764, Republic of Korea
[d] Fish Vaccine Development Center, Jeju National University, Jeju Self-Governing Province 690-756, Republic of Korea

ARTICLE INFO

Article history:
Received 11 March 2014
Received in revised form
10 June 2014
Accepted 13 June 2014
Available online 21 June 2014

Keywords:
TTRAP
Disk abalone
Gene ontology
Endonuclease activity
Transcriptional analysis

ABSTRACT

Immune signaling cascades have an indispensable role in the host defense of almost all the organisms. Tumor necrosis factor (TNF) signaling is considered as a prominent signaling pathway in vertebrate as well as invertebrate species. Within the signaling cascade, TNF receptor-associated factor (TRAF) and TNF receptor-associated protein (TTRAP) has been shown to have a crucial role in the modulation of immune signaling in animals. Here, we attempted to characterize a novel molluskan ortholog of TTRAP (AbTTRAP) from disk abalone (*Haliotis discus discus*) and analyzed its expression levels under pathogenic stress. The complete coding sequence of *AbTTRAP* consisted of 1071 nucleotides, coding for a 357 amino acid peptide, with a predicted molecular mass of 40 kDa. According to our *in-silico* analysis, AbTTRAP resembled the typical TTRAP domain architecture, including a 5′-tyrosyl DNA phosphodiesterase domain. Moreover, phylogenetic analysis revealed its common ancestral invertebrate origin, where AbTTRAP was clustered with molluskan counterparts. Quantitative real time PCR showed universally distributed expression of *AbTTRAP* in selected tissues of abalone, from which more prominent expression was detected in hemocytes. Upon stimulation with two pathogen-derived mitogens, lipopolysaccharide (LPS) and polyinosinic:polycytidylic acid (poly I:C), transcript levels of *AbTTRAP* in hemocytes and gill tissues were differentially modulated with time. In addition, the recombinant protein of AbTTRAP exhibited prominent endonuclease activity against abalone genomic DNA, which was enhanced by the presence of Mg^{2+} in the medium. Collectively, these results reinforce the existence of the TNF signaling cascade in mollusks like disk abalone, further implicating the putative regulatory behavior of TTRAP in invertebrate host pathology.

1. Introduction

Tumor necrosis factor (TNF)-related signaling is a highly complicated and tightly regulated process, in which members of TNF ligand and receptor family proteins specifically interact with each other to initiate and propagate a wide array of cascades to regulate multiple cellular events, including cell proliferation and differentiation, immune and inflammatory responses, and apoptosis [1]. In this regard, TNF receptor-associated factors (TRAFs) and adaptor proteins play a key role in transducing the initiated signals to mount respective immune responses, by changing the signaling molecules

* Corresponding authors. Marine Molecular Genetics Lab, Department of Marine Life Sciences, College of Ocean Science, Jeju National University, 66 Jejudaehakno, Ara-Dong, Jeju 690-756, Republic of Korea. Tel.: +82 64 754 3472; fax: +82 64 756 3493.
E-mail addresses: ilsonwhang@hanmail.net (I. Whang), jehee@jejunu.ac.kr, jeheedaum@hanmail.net (J. Lee).
[1] These authors have equally contributed to this work.

http://dx.doi.org/10.1016/j.fsi.2014.06.014
1050-4648/

within a target cell [2]. However, in order to render a vast array of cellular responses according to variety of stimuli, the activity of molecules in TNF signaling pathways are highly modulated through different regulatory factors, including TRAF family member-associated NF-kappa B activator (I-TRAF/TANK), TRAF-interacting protein (TRIP) and TRAF and TNF receptor-associated protein (TTRAP) [3–5]. Among these regulators, TTRAP plays a key role as a negative regulator of the nuclear factor κB (NF-κB) activation pathway through TNF signaling, as a result of interactions exerted with the cytoplasmic domain of CD40 and with TRAFs [4]. This further suppresses ever shorter telomere 1 (EST1) transcriptional activity and weakens synergistic transactivation by EST1 and activator protein 1 (AP1) as an E twenty-six transcription factor 1 (ETS-1)-associated protein [6]. On the other hand, overexpression of TTRAP could also trigger the activation of Janus kinase (JNK), leading to DNA fragmentation and apoptosis in human umbilical vein endothelial cells, as published in a previous report [7].

TTRAP is classified as a member of the Mg^{2+}/Mn^{2+}-dependent phosphodiesterase (MDP) superfamily, which includes sphingomyelinases, inositol-phosphatases and nucleases [8]. Among them, TTRAP is more closely related to nucleases than to sphingomyelinases or phosphatases [8]. TTRAP is known to share significant sequence and structure similarities with the human apurinic/apyrimidinic endonuclease (APE1), which is involved in both DNA repair and activation of transcription factors such as AP1 and p53 [9]. Interestingly, according to a previous report, endonuclease activity was empirically demonstrated in human TTRAP, where it was identified as a bona fide 3′- and 5′-tyrosyl DNA phosphodiesterase [10]. As suggested, this endonuclease activity was believed to be involved in DNA repair and apoptosis [11–13].

The identification and characterization of different regulatory molecules in TNF signaling pathways has been performed predominantly in vertebrates, particularly in mammals. However, reports on members of invertebrate TNF-related signaling cascades, especially mollusks are scarce, with the exception of reports on lipopolysaccharide (LPS)-induced TNF-α factor (LITAF), TNF-α and Fas ligand from *Haliotis discus discus* [14–16], and two TNF ligands, LITAF and TTRAP, exclusively from *Chlamys farreri* [17–20].

Abalones (*Haliotis* species) are marine gastropods that are cultivated as aqua-crops, contributing to an eminent proportion of the yield in commercial aquaculture industry in East and Southeast Asia. However, environmental stresses in their natural habitats, mostly from a wide range of pathogenic infections, have a negative impact on their survival and growth. Abalones are known to be infected by bacteria [21,22], viruses [23] and some parasites [24]. Nevertheless, the innate immune mechanisms functioning in abalones can combat these pathogenic threats to a certain extent. Therefore, revealing the mechanisms that exist in abalones is a constructive way to further develop appropriate strategies for their disease management.

In this study, an invertebrate ortholog of TTRAP from disk abalone (*H. discus discus*) (*AbTTRAP*) was identified and molecularly characterized, further analyzing its transcriptional modulation upon pathogen-derived mitogen stimulation. Furthermore, we demonstrated the endonuclease activity of AbTTRAP, using its purified recombinant protein, which is a typical functional property of TTRAPs, previously reported from invertebrates as well as vertebrates.

2. Materials and methods

2.1. Identification and sequence characterization

A cDNA library of disk abalone was constructed as described in our previous report [25]. A single putative clone, the sequence of which showed higher similarity to known TTRAP homologs, was identified using the Basic Local Alignment Tool (BLAST) algorithm (http://www.ncbi.nlm.nih.gov/BLAST). Subsequently, the DNA clone (containing TTRAP cDNA of disk abalone) was isolated using *AccuPrep*® Plasmid Mini Extraction kit (Bioneer, Korea). The *AbTTRAP* internal sequencing primer, TTRAP-I1 (Table 1), was designed based on the 3′-end of the known sequence, and then sequencing was carried out by ABI3700 sequencer (Macrogen, Korea). Finally, the full-length cDNA sequence of *AbTTRAP* in disk abalone was identified. The coding sequence and respective amino acid sequence of AbTTRAP were derived using DNAssist 2.2 software (www.DNAssist.org).

Characteristic domains and sequences existing in TTRAP molecules were predicted in AbTTRAP protein sequence using the NCBI-CDD server (http://www.ncbi.nlm.nih.gov/Structure/cdd/wrpsb.cgi) [26] and SMART online server (http://smart.embl-heidelberg.de). In order to compare the derived AbTTRAP protein sequence with its orthologs, pairwise sequence alignments and multiple sequence alignment were performed using emboss needle (http://www.Ebi.ac.uk/Tools/emboss/align) and ClustalW2 (http://www.Ebi.ac.uk/Tools/clustalw2) online programs, respectively. In addition, some of the physicochemical properties of AbTTRAP were determined through DNAssist 2.2 software. The phylogenetic relationship of AbTTRAP with its orthologous sequences was determined using the Neighbor-joining method under bootstrapping values taken from 1000 replicates by Molecular Evolutionary Genetics Analysis (MEGA) software version 5 [27].

2.2. Prediction of protein function

In order to improve the accuracy of our *in-silico* predictions, domain analysis, biological processes and molecular functions associated with AbTTRAP were further annotated using gene ontology (GO) hierarchical prediction by using the I-TASSER online server and COFACTER algorithm [28,29], which simulates the derived AbTTRAP protein sequence.

2.3. Generation of a recombinant AbTTRAP plasmid construct

The coding sequence of *AbTTRAP* was PCR-amplified and cloned into the pMAL-c2X vector, as described in the protocol of pMAL™ Protein Fusion and Purification System (New England Biolabs, UK), resulting a recombinant plasmid construct. Briefly, the open reading frame (ORF) of AbTTRAP gene was amplified using the sequence-specific primers, AbTTRAP-EF and AbTTRAP-ER, consisted with the restriction enzyme sites for *Eco*RI and *Hin*dIII, respectively (Table 1). PCR was performed in a TaKaRa thermal

Table 1
Primers used in the study. F and R refer to forward and reverse oligomers, respectively.

Name	Target	Primer sequence (5′–3′)
TTRAP-I1	Internal sequencing	CAGAATGTATCATTGCCTCCAGGAT
AbTTRAP-F	Real time PCR amplification	AAATGTCGTGTGAAGGGCATCAGC
AbTTRAP-R	Real time PCR amplification	AGTGTCGCCACCGAATATGACAG
AbTTRAP-EF	ORF cloning for expression	gagagaGAATTCTCTGACAGTGAGGCTGACAGTG
AbTTRAP-ER	ORF cloning for expression	gagagaCTGCAGCTAGACTGACGCACAGGTTGG
AbRibosomal-F	Real time PCR amplification	GGGAAGTGTGGCGTGTCAAATACA
AbRibosomal-R	Real time PCR amplification	TCCCTTCTTGGCGTTCTTCCTCTT

cycler in a total volume of 50 μL with 5 U of Ex Taq™ Polymerase (TaKaRa, Japan), 5 μL of 10× Ex Taq™ buffer, 8 μL of 2.5 mM dNTPs, 80 ng of template, and 20 pmol of each primer. The reaction was carried out in 35 cycles under the following conditions: 94 °C for 30 s, 56 °C for 30 s and 72 °C for 1 min, along with a final extension at 72 °C for 5 min. The PCR product (approximately 1.6 kbp) was resolved on a 1% agarose gel, excised, and purified using the *Accuprep*™ gel purification kit (Bioneer Co., Korea). The digested pMAL-c2X vector (150 ng) and PCR product (180 ng) were ligated using Mighty Mix (7.5 μL, TaKaRa, Japan) at 4 °C overnight. The ligated pMAL-c2X/AbTTRAP product was transformed into DH5α cells and sequenced. The sequence-confirmed recombinant expression plasmid was transformed into *Escherichia coli* BL21 (DE3) competent cells.

2.4. Overexpression and purification of recombinant AbTTRAP (rAbTTRAP)

The recombinant AbTTRAP protein as a fusion product with maltose binding protein (MBP - rAbTTRAP) was overexpressed using isopropyl-β-galactopyranoside (IPTG, 1 mM final concentration) at 20 °C for 16 h in *E. coli* BL21 (DE3) cells carrying the recombinant fusion construct. Subsequently, the protein was purified using the pMAL protein fusion and purification system. The purified protein was eluted with elution buffer (10 mM maltose) and the concentration was determined by the Bradford method using bovine serum albumin (BSA) as the standard [30]. The rAbTTRAP samples collected from different purification steps were analyzed by SDS-PAGE, using 12% gels under reduced conditions, with standard molecular weight marker (TaKaRa, Japan). This confirmed the successful overexpression of rAbTTRAP, along with the sufficient purity and integrity of the final eluted fusion protein, after staining the gel with 0.05% Coomassie blue R-250, followed by a standard de-staining procedure.

2.5. Investigation of the endonuclease activity of rAbTTRAP

In order to analyze the endonuclease activity of AbTTRAP and its dependence on the presence of Mg^{2+}, genomic DNA (gDNA) of disk abalone was digested with the purified rAbTTRAP fusion protein. Disk abalone gDNA was extracted from its muscle tissues using QIAamp DNA Mini Kit (QIAGEN-USA) according to the manufacturer's instructions. Extracted DNA was incubated with 100 μg of rAbTTRAP fusion protein in Tris-HCl, with or without adding $MgCl_2$ (Final concentration - 5 mM), 37 °C for 2, 4 and 8 h. Abalone DNA was also mixed with 100 μg of MBP instead of rAbTTRAP, as a control, and incubated at 37 °C for 8 h to clarify the effect of MBP fusion on the endonuclease activity of rAbTTRAP. After the relevant period of digestion, reaction mixtures were analyzed by 1% agarose gel electrophoresis, to observe the degree of DNA cleavage.

2.6. Animal rearing and tissue collection

Pre-acclimatized (1 week) unchallenged disk abalones (*H. discus discus*) averaging 8 cm in size were obtained from the "Youngsoo" abalone farm (Jeju Island, Korea). The seawater was filtered and aerated continuously; salinity and temperature were maintained at 34 ± 1‰ and 20 ± 1 °C, respectively. Abalones were fed daily with fresh marine seaweed (*Undaria pinnatifida*) during the acclimation period. Hemolymph was collected from pericardial cavities of three healthy and unchallenged animals, using sterilized syringes separately, and samples were immediately centrifuged (3000 *g* at 4 °C for 10 min) to harvest the hemocytes. Tissues from adductor muscle, mantle, gill, hepatopancreas, digestive tract, brain and gonad were collected from three animals, snap frozen in liquid nitrogen and stored at −80 °C.

2.7. Stimulation of healthy abalones with pathogen-derived mitogens

Abalones with an average weight of 50 g and average size of 8 cm were selected for the immune challenge experiment. One group of collected abalones was intramuscularly injected with 100 μL (500 μg/animal) of LPS in saline, equaling a dose of approximately 10 mg/kg (*E. coli* 0127:B8, Sigma-Aldrich, USA). In order to expose abalones to a viral mitogen stress, healthy animals were injected with 100 μL (10 μg/μL) of polyinosinic:polycytidylic acid (poly I:C) (Sigma-Aldrich, USA) in saline. A group of abalones that had not been injected was used as a negative control, and another group of abalones injected with the same amount of saline was kept as an alternative negative control. Hemolymph was extracted and hemocytes were collected from both control and challenged groups at respective time points, as described in Section 2.6. Gill tissues were also collected from both groups at 3, 6, 12, 24, 48, and 72 h post-injection. Total RNA was extracted from the corresponding tissues of at least four animals and used for cDNA synthesis.

2.8. Total RNA extraction and cDNA synthesis

Total RNA was extracted by Tri-Reagent™ (Sigma-Aldrich, USA) from abalone muscle, mantle, gill, hemocytes, digestive tract, hepatopancreas, and gonad of healthy animals, as well as from the collected gill tissues of immune-stimulated abalones. Concentration was quantified by measuring the absorbance at 260 nm in a UV spectrophotometer (Bio-Rad, USA). Purified RNA samples were diluted up to 1 μg/μL and subjected to cDNA synthesis through reverse transcription PCR using the PrimeScript™ cDNA Synthesis Kit (TaKaRa, Japan), following the manufacturer's instructions. Finally, newly synthesized cDNA was diluted 40-fold (800 μL total) before storing at −20 °C until further analysis.

2.9. Transcriptional analysis of AbTTRAP by quantitative real time PCR (qPCR)

qPCR was used to detect the expression levels of *AbTTRAP* in tissues of unchallenged abalones, and the temporal expression of *AbTTRAP* in gills and hemocytes of immune-stimulated animals. Total RNA was extracted at different time points following the immune stimulation, and first strand cDNA synthesis was carried out as described in Section 2.8. qPCR was performed using the Dice™ (Real Time System TP800, TaKaRa, Japan) thermal cycler, in a 15 μL reaction volume containing 4 μL of diluted cDNA from each tissue, 7.5 μL of 2× TaKaRa Ex-Taq™ SYBR Green Premix, 0.6 μL of each primer (AbTTRAP-F and AbTTRAP-R) (Table 1) and 2.3 μL of dH_2O. qPCR was carried out under the following conditions: 95 °C for 10 s, then 35 cycles of 5 s at 95 °C, 10 s at 58 °C and 20 s at 72 °C, and a final cycle of 95 °C for 15 s, 60 °C for 30 s and 95 °C for 15 s. The baseline was set automatically by the Dice™ thermal cycler Real Time System Software (Version 2.00) (TaKaRa, Japan). *AbTTRAP* expression was determined by the Livak ($2^{-\Delta\Delta Ct}$) method [31]. The same qPCR cycle profile was used for the internal control gene, abalone ribosomal protein L5 gene (GenBank ID: EF103443), using corresponding primers (AbRibosomal-F, AbRibosomal-R, Table 1). Expression levels were analyzed in triplicate, and all of the data were presented as relative mRNA expression by calculating the mean ± standard deviation (SD). The transcript levels detected following each stimulant were compared with expression levels of the internal reference gene, and further normalized to the

```
  GGGGCTAGACAGGCGGGAGTGATATCAAACATGTCGGTCGATTAAGTCTGAATCAAAA   −181
GTGTAGTTATTTCACAACAACAAGGCAGTGTCGGCACAAAAGAAGCACTTGAAGTAAACA   −121
AGTCCTGGTCAATTACACATTAGCCTATGTCAGAGGCTATTGCGTATTGCATGTTTTAAT   −61
CGTAGCAGCTCCTTGAGTGGATCTCAACACTACTGCGTAGATCTCCCCAGCAGCCGCAGG   −1
ATGTCTGACAGTGAGGCTGACAGTGATGTGGATGAGAAGAATCTCCCTTCCAGGGAGGAG   60
 M  S  D  S  E  A  D  S  D  V  D  E  K  N  L  P  S  R  E  E    20
TGCGAGGAGAGATGTCAGATGTTCGCCCAAGTGACCGGCACCGACACTGCTCTAGCCATG   120
 C  E  E  R  C  Q  M  F  A  Q  V  T  G  T  D  T  A  L  A  M    40
TTCTATCTTCAAGATAGGGAATGGAACGTAGAGACAGCACTGAATGCTTATTTCGCAGAG   180
 F  Y  L  Q  D  R  E  W  N  V  E  T  A  L  N  A  Y  F  A  E    60
ACGGGGGGTGAACCAGTGGGGTCAGGTCAGAACACCATCGTTGGCACCAACACACATAGC   240
 T  G  G  E  P  V  G  S  G  Q  N  T  I  V  G  T  N  T  H  S    80
AGAACACAAACAGTGAGAGCTGGACCGGAAGGACCTGATCCAGAGCCTCACCGTATCCGC   300
 R  T  Q  T  V  R  A  G  P  E  G  P  D  P  E  P  H  R  I  R   100
CTCTTGTCCTGGAACCTGGATGGCCTTGACCCTGGGAGCATCAAGTCCAGGATGCAAGCT   360
 L  L  S  W  N  L  D  G  L  D  P  G  S  I  K  S  R  M  Q  A   120
GTTTGTGACATCATTAACAAGGAGAAGCCCCACGTAGTGTTCCTCCAGGAAGTGACCCCC   420
 V  C  D  I  I  N  K  E  K  P  H  V  V  F  L  Q  E  V  T  P   140
CTCACCCTCCCTATCCTGGAGGATGGGTGCGGCATGTACCAGGTGATCCCAGGGGGAGAC   480
 L  T  L  P  I  L  E  D  G  C  G  M  Y  Q  V  I  P  G  G  D   160
AACCACTACTTCACTGCTATCATGCTGCGGGTTGGACATGTACAGTTTGAAGATGCTGTG   540
 N  H  Y  F  T  A  I  M  L  R  V  G  H  V  Q  F  E  D  A  V   180
GTTACATCCTTCCCAACCAGCAAGATGTTGAGAAACATTATAACAATCAAATGTCGTGTG   600
 V  T  S  F  P  T  S  K  M  L  R  N  I  I  T  I  K  C  R  V   200
AAGGGCATCAGCTTCCAGGTGATGACTTCCCACCTGGAGAGTACGGCTGCGCACAGTGAT   660
 K  G  I  S  F  Q  V  M  T  S  H  L  E  S  T  A  A  H  S  D   220
GAGAGGAAGAGGCAGTTGGTACGGGCATTCGAGGCGATGAAACACGCAGATCCTGACAGA   720
 E  R  K  R  Q  L  V  R  A  F  E  A  M  K  H  A  D  P  D  R   240
ACTGTCATATTCGGTGGCGACACTAACCTGAGAGATAAGGAGGTGGCCCAGGTTGGAGGT   780
 T  V  I  F  G  G  D  T  N  L  R  D  K  E  V  A  Q  V  G  G   260
ATCCCGGAAGATATCTACGACATATGGGAGATGACGGGCCAGCGTCCAGAGGCCAAGTTC   840
 I  P  E  D  I  Y  D  I  W  E  M  T  G  Q  R  P  E  A  K  F   280
ACCTGGGACATGAGGAGAAACGACAACCATGAATACCCAGGATACAAATCATTCCTGAGA   900
 T  W  D  M  R  R  N  D  N  H  E  Y  P  G  Y  K  S  F  L  R   300
CCGGACCGACTTTACATCCGTCATTGTAAGCCCAGATCCAAAGTGACCCCCGTGTACTTC   960
 P  D  R  L  Y  I  R  H  C  K  P  R  S  K  V  T  P  V  Y  F   320
GAACTGACTGGTCTCGCTCGACTCCCCAGCAACAAGTTTCCCAGCGATCACTGGGGGCTT  1020
 E  L  T  G  L  A  R  L  P  S  N  K  F  P  S  D  H  W  G  L   340
CTGGCACACTTTGACATCAATGGCGTTTCCAAGCCAACCTGTGCGTCAGTCTAGCCGTTC  1080
 L  A  H  F  D  I  N  G  V  S  K  P  T  C  A  S  V  *         357
ACATCACACACCTTGGAGTCCTTGTTGATTATCATTGTCTATGTGTGAAAAGTAATCAGC  1140
ATTTCCAAGTTAGATTAATTGTTATGTCAAGCATTTGATCAGAATGTATCATTGCCTCCA  1200
GGATAGAAATGTTTAAAGATCACTGGATTGATCAGAGAATCATTTTTGTAAAATATTTGT  1260
TTGTTGAAAAAGTGGACAGTTCATTTGCCATGTGGAGATATATTCTTGTTTCTGCTGTTG  1320
AGATTTCAACATTGTCTACTTACTTAAGCTGAGAGTAAAACACCTGATTTGATTGTTGTC  1380
AATATTTATGATTGGGATATTTACCCTTTCACAAGAAAATATATCTCATTGACAGATTGT  1440
ATGATTATTGTGTTATCATCAGGGGTGAGAATCTGCCGCGGATCTACGAATTTCCGTGAA  1500
TTTTAGTGACGACAAATTTTGTCAAAATCTGATGGCTTAAAGGTCAAACTCCACTTATCT  1560
CCCATAAACACCCCCAAATTATGGCACACGCTTCATTGAAAAAAAAAAAAAAAAAAAAAA  1599
```

Fig. 1. Nucleotide and deduced amino acid sequence of *AbTTRAP*. The start codon (ATG), the stop codon (TGA), RNA instability motifs (ATTTA) and poly (A) tail are shown in bold. The *in-silico* predicted 5′-tyrosyl DNA phosphodiesterase domain is shaded in gray. The residues in putative catalytic sites are denoted using discontinuous boxes, in which putative phosphate binding residues and metal binding resides are indicated in bold and italic, respectively.

expression levels of corresponding saline-injected controls at each time point post-injection. In addition, the relative transcript level of a non-injected control (0 h) group was defined as the basal expression level in each experiment. To determine the statistical significance ($P < 0.05$) between each experimental group and the negative control group (non-injected animals), two-tailed unpaired *t*-tests were performed.

3. Results and discussion

3.1. Sequence profiles of AbTTRAP

The complete cDNA sequence (1860 bp) of *AbTTRAP*, consisted of a 1071 bp ORF sequence coding for a 357-amino acid peptide, a 238 bp 5′-untranslated region (5′-UTR) and a 551 bp 3′-UTR. The complete cDNA sequence of *AbTTRAP* was deposited in the GenBank database under the accession number JQ710444. According to the *in-silico* prediction, the molecular mass of AbTTRAP protein was around 40 kDa and the theoretical isoelectric point was around 5.6. As anticipated by bioinformatic tools, AbTTRAP displayed the conserved features of typical TTRAP molecules, suggesting that AbTTRAP is indeed an ortholog of TTRAPs. These features include a 5′-tyrosyl DNA phosphodiesterase domain (TDP domain, residues 100–344), which was commonly identified in proteins involved in intracellular signaling and particularly in Mg^{2+}/Mn^{2+}-dependent phosphodiesterases [8], putative catalytic sites (residues 105, 137, 211, 147, 149, 302, 336 and 337), putative metal binding sites (residues 137 and 336) and putative phosphate binding sites (residues 211 and 337) (Fig. 1).

3.2. Anticipated functions of AbTTRAP via gene ontology analysis

According to the hierarchical prediction of gene ontology, in terms of molecular function and biological process, AbTTRAP protein was anticipated to bind metal ions and be involved in cell death, respectively, under adequate levels of GO-score (0.74 and 0.53, respectively). This was calculated based on the average weight of global and local similarity between query and template proteins. As shown in Fig. 2(A), graphical representation depicts the hierarchy of predicted molecular functions of AbTTRAP based on the corresponding GO terms of templates, in which ultimately the function has reduced to metal ion binding. This anticipation reinforces the presence of putative iron binding sites in AbTTRAP protein sequence, as predicted in our computational analysis, which is consistent with the Mg^{2+}/Mn^{2+} dependence of typical TTRAP function [8]. Furthermore, the GO annotation predicted the putative involvement of AbTTRAP in cell death processes, which is consistent with the distinct functional role of known TTRAPs, since they can suppress the activation of NF-κB in the TNF signaling pathway to activate JNK-mediated apoptosis and DNA degradation in cells [4,7].

3.3. Sequence homology between AbTTRAP and its orthologs

According to the pairwise sequence alignment study, AbTTRAP exhibited the highest percent identity (45.5%) and similarity (60.3%) values when compared with its counterpart from the invertebrate, *C. farreri*, and the lowest percent identity (25.6%) and similarity (39.6%) when compared with its counterpart from the vertebrate, *Oreochromis niloticus* (Table 2). As shown in Fig. 3, multiple sequence alignment of AbTTRAP with its orthologs revealed the conservation of four motifs important for endonuclease activity in AbTTRAP. These motifs are known to be involved in the maintenance of orientation of catalytic residue (S/TWN), coordination of the cofactors Mg^{2+} or Mn^{2+} (LQE), interactions with phosphate groups of the substrate (GDXN), as well as acid-base catalysis and stabilizing the transition state (SDH), as characterized in mammals and prokaryotes [13,32].

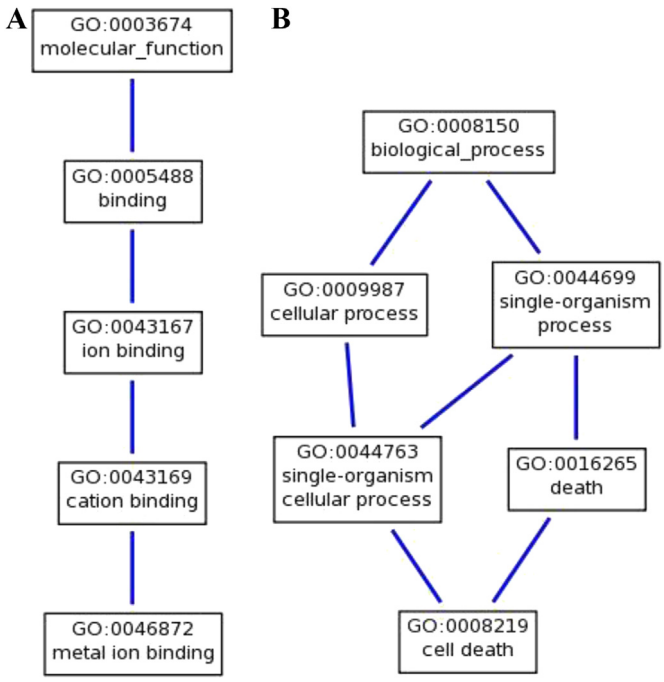

Fig. 2. Gene ontology hierarchy of AbTTRAP functions. (A) Graphical representation of predicted AbTTRAP molecular function, with respect to the GO terms of template proteins. (B) Graphical representation of the biological processes in which AbTTRAP is putatively involved.

3.4. Phylogenetic reconstruction of AbTTRAP

Phylogenetic analysis of AbTTRAP protein sequence, with its different vertebrate and invertebrate counterparts confirmed its invertebrate ancestral origin, since it was sub-clustered with a mollusk species, *C. farreri*, showing strong bootstrapping support (99) under the main invertebrate clade (Fig. 4). Vertebrate TTRAPs were clustered separately in a large clade, where mammalian and fish counterparts were sub-grouped together as expected, reflecting an accepted evolutionary relationship. Notably, the TTRAP ortholog of the nematode parasite, *Trichinella spiralis*, showed a distant evolutionary relationship with the other vertebrate and invertebrate clades, clustering outside of the main branch of the tree.

3.5. Endonuclease activity of rAbTTRAP

TTRAPs are known as key regulatory factors involved not only in TNF signaling, but are also in the efficient repair mechanisms of

Table 2
Percent identity and similarity of AbTTRAP with its orthologs.

Species	Identity	Similarity	GenBank accession no.
Chlamys farreri	45.5	60.3	ACS72243
Saccoglossus kowalevskii	39.5	54.1	XP_002732161
Heterocephalus glaber	34.8	48.9	EHB09596
Anolis carolinensis	38.5	50.9	XP_003219821
Meleagris gallopavo	36.8	51.3	XP_003204960
Xenopus laevis	34.1	49.4	NP_001092156
Danio rerio	33.2	50.2	CAK05007
Cavia porcellus	34.6	49.2	XP_003468816
Lepeophtheirus salmonis	32.9	48.9	ADD38656
Homo sapiens	31.2	44.8	EAW55458
Oreochromis niloticus	25.6	39.6	XP_003444211

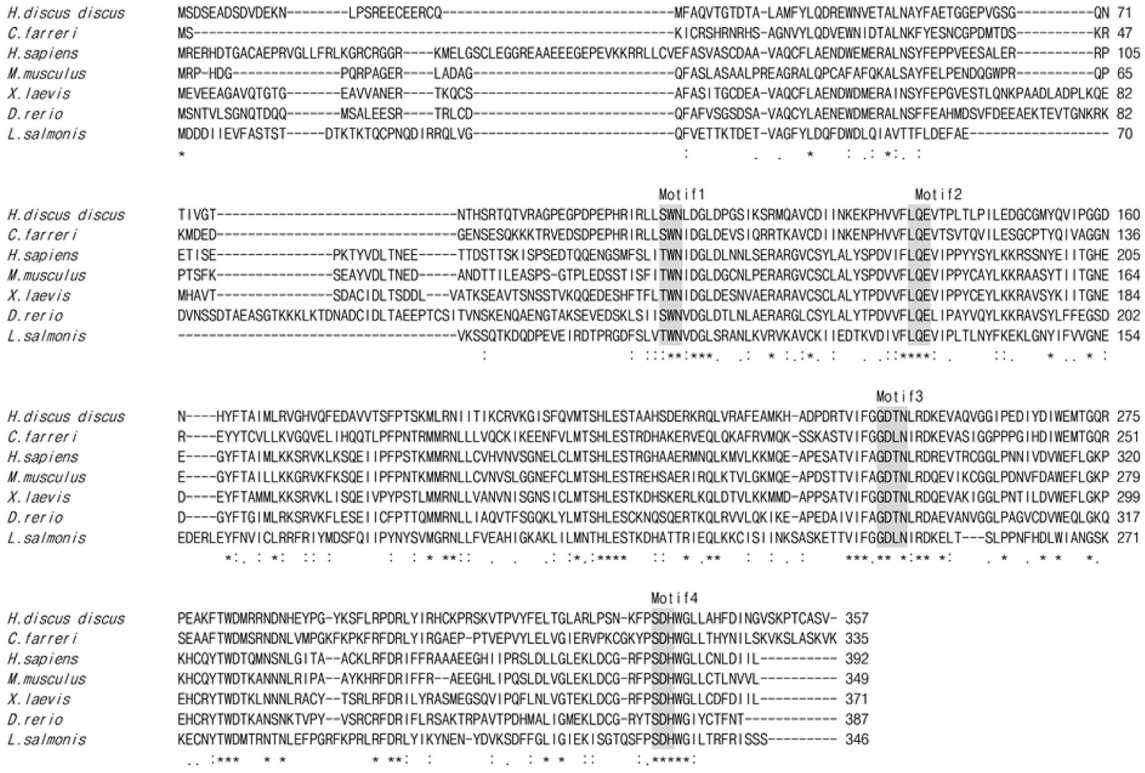

Fig. 3. Multiple sequence alignment of different vertebrate and invertebrate TTRAP counterparts. Completely conserved residues are denoted by an asterisk under the corresponding alignment. Four conserved motifs known to be involved in the proper orientation of catalytic residues (Motif 1), coordination of Mg^{2+} or Mn^{2+} ions (Motif 2), interactions with the phosphate group of the substrate (Motif 3), and acid-base catalysis and stabilization of the transition state (Motif 4) are shaded in gray.

topoisomerase II (Top2)-induced chromosomal double-strand breaks, through their potent Mg^{2+}/Mn^{2+}-dependent 5′-tyrosyl DNA phosphodiesterase activity [10]. Therefore, the potential endonuclease activity of purified rAbTTRAP against abalone genomic DNA was analyzed. Agarose gel electrophoretic analysis of the reaction mixtures revealed the clear nuclease activity of rAbTTRAP through degradation of abalone genomic DNA with the time. This demonstrated the characteristic function of TTRAPs, even in the absence of Mg^{2+}, and activity was increased by the presence of Mg^{2+} (Fig. 5, lanes 3–8). However, no digestion was observed for the MBP control, indicating its dormant behavior within the rAbTTRAP fusion product. A similar functional property has already been identified in a TTRAP ortholog of *C. farreri*, as the only evidence from mollusk species other than disk abalone, in which detectable endonuclease activity was only observed in the presence of Mg^{2+}, reinforcing its importance in DNA repair mechanisms [20].

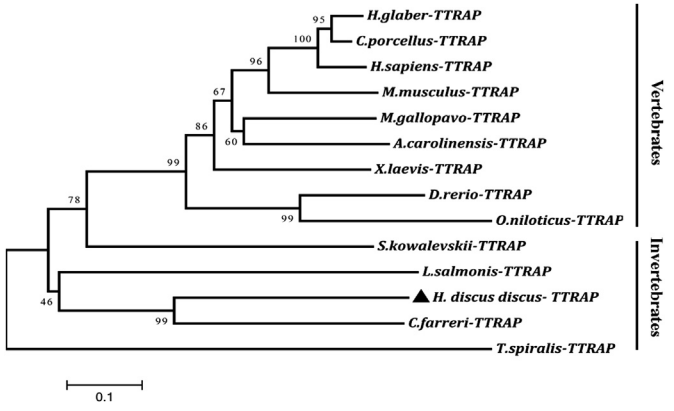

Fig. 4. Phylogenetic analysis of AbTTRAP. The tree was constructed based on ClustalW alignment of the deduced amino acid sequences of different vertebrate and invertebrate orthologs estimated by the Neighbor-joining method in MEGA version 5.0. Bootstrap values are shown for each lineage of the tree, at respective branches. The NCBI-GenBank accession numbers are given in Table 2, except for *M. musculus* (EDL32474) and *T. spiralis* (XP_003368460).

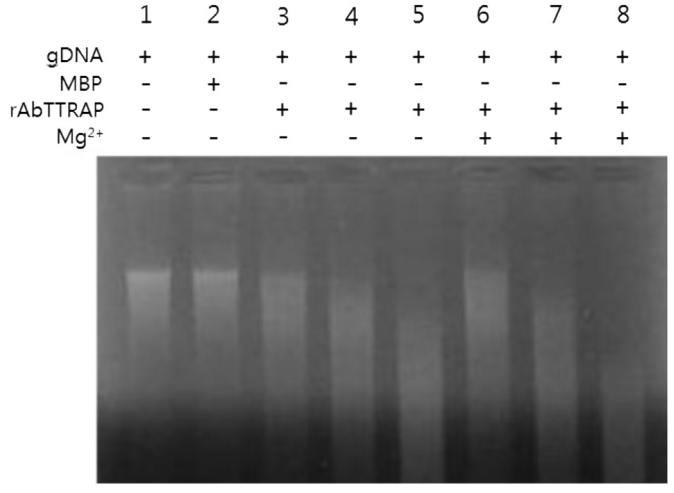

Fig. 5. In vitro rAbTTRAP endonuclease activity against abalone genomic DNA (gDNA). Degradation of 100 μg of disk abalone gDNA by rAbTTRAP with the presence or absence of 5 mM Mg^{2+} was analyzed using agarose gel-elecrophoresis. The reagents used in each treatment were indicated above the respective lanes corresponding to the each experiment. The incubation time after treatment at corresponding assay was 8, 8, 2, 4, 8, 2, 4, 8 in hours, lane 1 to 8, respectively.

3.6. Spatial mRNA expression pattern

In order to prefigure the importance of AbTTRAP in abalone physiology as a key regulatory element in TNF receptor-associated signaling pathways, the tissue-specific mRNA expression profile of *AbTTRAP* was investigated in some of the physiologically important tissues of disk abalone, using qPCR. Consistent with previously observed transcriptional profiles in human [4] and the mollusk, *C. farreri* [20], *AbTTRAP* transcription was ubiquitously distributed among the tissues examined, albeit in different magnitudes, confirming its universal importance in the cellular processes of abalone (Fig. 6). The highest transcript level of *AbTTRAP* was detected in abalone hemocytes, whereas the lowest was observed in muscle. This contrasted the expression profile of the TTRAP homolog in *C. farreri*, where expression was more pronounced in muscle and diminished in hemocytes. However, the abundant level of *AbTTRAP* transcripts in hemocytes may be attributed to its immune modulatory properties, especially with respect to TNF receptor signaling, since hemocytes function as a major innate immune component in mollusk species such as abalones, through involvement in phagocytosis-like cellular processes [33].

3.7. Modulated transcription of AbTTRAP under pathogenic stress

With the objective of investigating the potential modulation of host defense by AbTTRAP, its temporal mRNA expression level in hemocytes and gill tissues was measured by qPCR, upon stimulation with the well-characterized bacterial endotoxin, LPS, and double-stranded viral RNA emulator, poly I:C. The relative transcript level of *AbTTRAP* in hemocytes was significantly up-regulated ($P < 0.05$) in the early phase (3 h and 6 h) after LPS stimulation, but significantly down-regulated ($P < 0.05$) in its latter phase (12–48 h post-injection (p.i.)) (Fig. 7(A)). On the other hand, upon poly I:C stimulation, the *AbTTRAP* basal transcript level in hemocytes was initially down-regulated at 3 h, 12 h and 24 h p.i., and then elevated at 48 h p.i. in the later phase of the experiment (Fig. 7(A)). This contrasting observation may be attributed to the activation of two different immune signaling cascades in TNF signaling, upon two different pathogen-associated molecular patterns (PAMPs). Bacterial PAMPs such as LPS, which is characterized as a potent stimulator of TNF and the TNF receptor signaling pathway [34], may trigger the inhibition of TRAF-mediated activation of NF-κB, resulting in switching from the main TNF signaling pathway to JNK

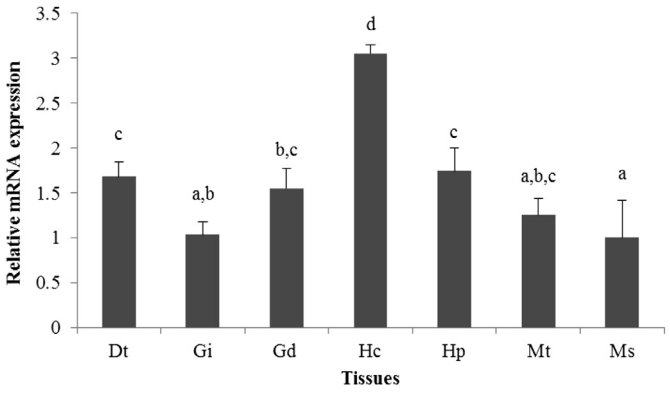

Fig. 6. Tissue-specific expression of *AbTTRAP* mRNA, as detected using quantitative real-time PCR (qPCR). Error bars represent standard deviation ($n = 3$). Data with different letter combinations represent statistically significant ($P < 0.05$) differences in transcript levels. Dt: digestive tract; Gi: gill; Gd: gonad; Hc: hemocytes; Hp: hepatopancreas; Mt: mantle; Ms: muscle.

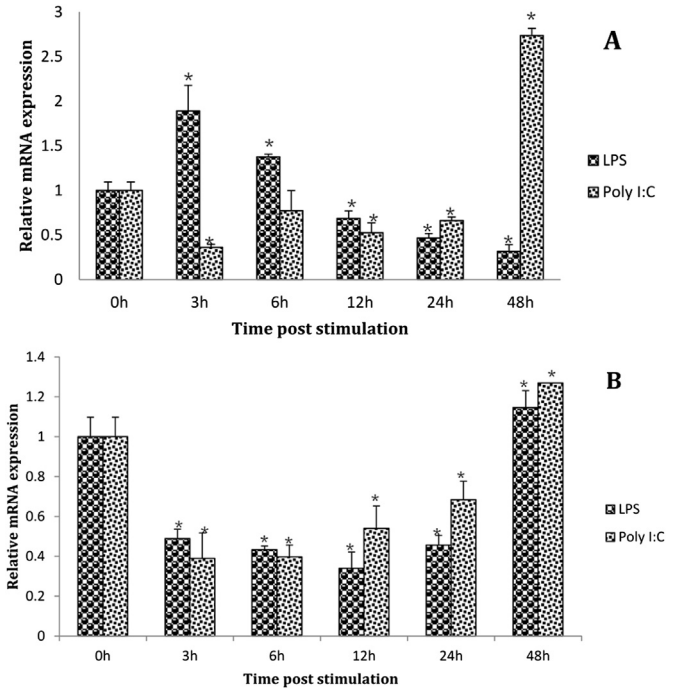

Fig. 7. Modulated transcriptional profiles of *AbTTRAP* in hemocytes (A) and gill tissue (B) upon LPS and poly I:C stimulation, as determined by quantitative real-time PCR (qPCR). Relative expression was calculated by the $2^{-\Delta\Delta Ct}$ method, using abalone ribosomal protein L5 as the reference gene with respect to the corresponding saline-injected controls at each time point. The relative expression fold-change at 0 h post-injection (Un-injected control) was used as the baseline. Error bars represent standard deviation ($n = 3$), and each asterisk indicates $P < 0.05$.

activation and causing apoptosis in the early phase of the infection [7]. However, it may also activate NF-κB, mediated by TRAF, to mount immune responses against bacterial pathogens in the late phase of the infection [4], which is reflected in the early phase up-regulated and late phase down-regulated transcript levels of *AbTTRAP*. In the case of poly I:C stimulation, activation of the aforementioned pathways may be triggered in an opposite manner, implicating the induction of NF-κB-mediated immune responses as the major defense strategy used against viral infection, through the TNF signaling cascade.

In contrast to the observed variation in hemocytes, the *AbTTRAP* mRNA expression level in gill (Fig. 7(B)) was modulated in a similar manner upon both LPS and poly I:C exposure, showing significant reduction ($P < 0.05$) from 3 h to 24 h p.i., with a single elevation above the basal level after 48 h. This may indicate the activation of NF-κB to evoke innate immune responses against invading pathogens [35] at the early phase and prior late phase of bacterial and viral infections [4], with a latter late phase induction of JNK-mediated apoptosis [7].

In terms of the clearance of damaged and pathogen-infected cells without mounting any inflammatory reactions, apoptosis plays a significant role in molluskan defense mechanisms against invading pathogens. In this regard, hemocytic apoptosis can be considered as an indispensable mechanism, triggered by pathogenic stress such as bacterial infection [36]. Therefore, the up-regulated transcriptional profile of *AbTTRAP* in hemocytes in the early phase after LPS stimulation may indicate the activation of apoptosis and DNA degradation in hemocytes following a bacterial (particularly gram-negative) infection. Meantime, observed expressional modulation in hemocytes showed marked difference compared to that observed in abalone gill tissue upon LPS stimulation. However, the transcriptional modulation of TTRAP in

abalone gill tissues and hemocytes reflects the prolonged activation of NF-κB under viral or bacterial PAMP stress, albeit in a different phase after stimulation. This implicates the immune modulatory properties of AbTTRAP upon bacterial or viral exposure, supporting to our previous evidence which confirms the existence of the TNF signaling pathway in disk abalone [14,15].

A previous study on molluskan TTRAP from *C. farreri* also reported that TTRAP transcription could be modulated by three different PAMPs, including β-glucan, LPS and peptidoglycan (PGN) [20]. In this case, LPS stimulation triggered a down-regulated expression profile in *C. farreri* hemocytes, which was consistent with the late-phase expression profile of *AbTTRAP* observed here upon LPS stimulation. However, the other PAMPs could induce significant elevations throughout the experiment, providing molecular insights into the TTRAP-modulated TNF signaling that exists in the molluskan level of invertebrate lineages. Nevertheless, in order to elucidate the exact mechanisms of TNF signaling in mollusks, further investigation has to be conducted, following the identification of different downstream members in a wide array of species.

4. Conclusion

Collectively, our computational and expression data reveal that AbTTRAP is indeed an ortholog of TTRAPs involved in the regulation of TNF signaling in abalone. Furthermore, the detected nuclease activity of AbTTRAP against abalone gDNA, which was enhanced by the presence of Mg^{2+}, reflected the characteristic of TTRAP as a molecule that may be involved in DNA repair mechanisms. Altogether, we can suggest that AbTTRAP is a molecule possessing immune modulatory properties, which may be involved in a TNF-TNF receptor signaling cascade in the host defense under pathogenic stress, potentially participating in DNA repair mechanisms through its potent endonuclease activity.

Acknowledgment

This research was supported by Golden Seed Project, Ministry of Agriculture, Food and Rural Affairs (MAFRA), Ministry of Oceans and Fisheries (MOF), Rural Development Administration (RDA) and Korea Forest Service (KFS).

References

[1] MacEwan DJ. TNF receptor subtype signalling: differences and cellular consequences. Cell Signal 2002;14:477–92.
[2] Wajant H, Henkler F, Scheurich P. The TNF-receptor-associated factor family: scaffold molecules for cytokine receptors, kinases and their regulators. Cell Signal 2001;13:389–400.
[3] Dempsey PW, Doyle SE, He JQ, Cheng G. The signaling adaptors and pathways activated by TNF superfamily. Cytokine Growth Factor Rev 2003;14:193–209.
[4] Pype S, Declercq W, Ibrahimi A, Michiels C, Van Rietschoten JG, Dewulf N, et al. TTRAP, a novel protein that associates with CD40, tumor necrosis factor (TNF) receptor-75 and TNF receptor-associated factors (TRAFs), and that inhibits nuclear factor-kappa B activation. J Biol Chem 2000;275:18586–93.
[5] Verstrepen L, Carpentier I, Verhelst K, Beyaert R. ABINs: a20 binding inhibitors of NF-kappa B and apoptosis signaling. Biochem Pharmacol 2009;78:105–14.
[6] Pei H, Yordy JS, Leng Q, Zhao Q, Watson DK, Li R. EAPII interacts with ETS1 and modulates its transcriptional function. Oncogene 2003;22:2699–709.
[7] Lee HY, Youn SW, Kim JY, Park KW, Hwang CI, Park WY, et al. FOXO3a turns the tumor necrosis factor receptor signaling towards apoptosis through reciprocal regulation of c-Jun N-terminal kinase and NF-kappaB. Arterioscler Thromb Vasc Biol 2008;28:112–20.
[8] Rodrigues-Lima F, Josephs M, Katan M, Cassinat B. Sequence analysis identifies TTRAP, a protein that associates with CD40 and TNF receptor-associated factors, as a member of a superfamily of divalent cation-dependent phosphodiesterases. Biochem Biophys Res Commun 2001;285:1274–9.
[9] Zhou J, Ahn J, Wilson SH, Prives C. A role for p53 in base excision repair. EMBO J 2001;20:914–23.
[10] Cortes Ledesma F, El Khamisy SF, Zuma MC, Osborn K, Caldecott KW. A human 5′-tyrosyl DNA phosphodiesterase that repairs topoisomerase-mediated DNA damage. Nature 2009;461:674–8.
[11] Hofmann K, Tomiuk S, Wolff G, Stoffel W. Cloning and characterization of the mammalian brain-specific, Mg2+-dependent neutral sphingomyelinase. Proc Natl Acad Sci U S A 2000;97:5895–900.
[12] Tomiuk S, Hofmann K, Nix M, Zumbansen M, Stoffel W. Cloned mammalian neutral sphingomyelinase: functions in sphingolipid signaling? Proc Natl Acad Sci U S A 1998;95:3638–43.
[13] Whisstock JC, Romero S, Gurung R, Nandurkar H, Ooms LM, Bottomley SP, et al. The inositol polyphosphate 5-phosphatases and the apurinic/apyrimidinic base excision repair endonucleases share a common mechanism for catalysis. J Biol Chem 2000;275:37055–61.
[14] De Zoysa M, Nikapitiya C, Oh C, Whang I, Lee JS, Jung SJ, et al. Molecular evidence for the existence of lipopolysaccharide-induced TNF-alpha factor (LITAF) and Rel/NF-kB pathways in disk abalone (Haliotis discus discus). Fish Shellfish Immunol 2010;28:754–63.
[15] De Zoysa M, Jung S, Lee J. First molluscan TNF-alpha homologue of the TNF superfamily in disk abalone: molecular characterization and expression analysis. Fish Shellfish Immunol 2009;26:625–31.
[16] De Zoysa M, Nikapitiya C, Moon DO, Whang I, Kim GY, Lee J. A novel Fas ligand in mollusk abalone: molecular characterization, immune responses and biological activity of the recombinant protein. Fish Shellfish Immunol 2009;27:423–32.
[17] Li L, Qiu L, Song L, Song X, Zhao J, Wang L, et al. First molluscan TNFR homologue in Zhikong scallop: molecular characterization and expression analysis. Fish Shellfish Immunol 2009;27:625–32.
[18] Su J, Qiu L, Li L, Liu L, Wang L, Siva VS, et al. cDNA cloning and characterization of a new member of the tumor necrosis factor receptor family gene from scallop, Chlamys farreri. Mol Biol Rep 2011;38:4483–90.
[19] Yu Y, Qiu L, Song L, Zhao J, Ni D, Zhang Y, et al. Molecular cloning and characterization of a putative lipopolysaccharide-induced TNF-alpha factor (LITAF) gene homologue from Zhikong scallop Chlamys farreri. Fish Shellfish Immunol 2007;23:419–29.
[20] Yang J, Qiu L, Wang L, Huang M, Zhang H, Song L. A TRAF and TNF receptor-associated protein (TTRAP) in mollusk with endonuclease activity. Dev Comp Immunol 2011;35:827–34.
[21] Liu PC, Chen YC, Huang CY, Lee KK. Virulence of Vibrio parahaemolyticus isolated from cultured small abalone, Haliotis diversicolor supertexta, with withering syndrome. Lett Appl Microbiol 2000;31:433–7.
[22] Huang CY, Liu PC, Lee KK. Withering syndrome of the small abalone, Haliotis diversicolor supertexta, is caused by Vibrio parahaemolyticus and associated with thermal induction. Zeitschrift fur Naturforschung C J Biosci 2001;56:898–901.
[23] Nakatsugawa T, Nagai K, Hiya T, Nishizawa K, Muroga A. A virus isolated from juvenile Japanese black abalone Nordotis discus discus affected with amyotrophia. Dis Aquat Org 1999;36:159–61.
[24] Goggin RJG. Perkinsus L. a protistan parasite of abalone in Australia. Mar Freshw Res 1995;46:639–46.
[25] Lee Y, De Zoysa M, Whang I, Lee S, Kim Y, Oh C, et al. Molluscan death effector domain (DED)-containing caspase-8 gene from disk abalone (Haliotis discus discus): molecular characterization and expression analysis. Fish Shellfish Immunol 2011;30:480–7.
[26] Marchler-Bauer A, Lu S, Anderson JB, Chitsaz F, Derbyshire MK, DeWeese-Scott C, et al. CDD: a conserved domain database for the functional annotation of proteins. Nucleic Acids Res 2011;39:D225–9.
[27] Tamura K, Peterson D, Peterson N, Stecher G, Nei M, Kumar S. MEGA5: molecular evolutionary genetics analysis using maximum likelihood, evolutionary distance, and maximum parsimony methods. Mol Biol Evol 2011;28:2731–9.
[28] Roy A, Kucukural A, Zhang Y. I-TASSER: a unified platform for automated protein structure and function prediction. Nat Protoc 2010;5:725–38.
[29] Roy A, Yang J, Zhang Y. COFACTOR: an accurate comparative algorithm for structure-based protein function annotation. Nucleic Acids Res 2012;40:W471–7.
[30] Bradford MM. A rapid and sensitive method for the quantitation of microgram quantities of protein utilizing the principle of protein-dye binding. Anal Biochem 1976;72:248–54.
[31] Livak KJ, Schmittgen TD. Analysis of relative gene expression data using real-time quantitative PCR and the 2(-Delta Delta C(T)) method. Methods 2001;25:402–8.
[32] Matsuo Y, Yamada A, Tsukamoto K, Tamura H, Ikezawa H, Nakamura H, et al. A distant evolutionary relationship between bacterial sphingomyelinase and mammalian DNase I. Protein Sci – Publ Protein Soc 1996;5:2459–67.
[33] Glinski Z, Jarosz J. Molluscan immune defenses. Arch Immunol Ther Exp 1997;45:149–55.
[34] Beutler B, Milsark IW, Cerami AC. Passive immunization against cachectin/tumor necrosis factor protects mice from lethal effect of endotoxin. Science 1985;229:869–71.
[35] Hatada EN, Krappmann D, Scheidereit C. NF-kappaB and the innate immune response. Curr Opin Immunol 2000;12:52–8.
[36] Terahara K, Takahashi KG. Mechanisms and immunological roles of apoptosis in molluscs. Curr Pharm Des 2008;14:131–7.